Investigation of Cable Influence on the Interturn Transient Voltage Distribution in Rotating Machine Windings using a Three-Phase Model

R. S. Ferreira, A. C. Ferreira

***Abstract*—Turn-to-turn and turn-to-ground transient voltages due to the surges which arrive at rotating machine terminals shall be known as exactly as possible to optimize the insulation design. Normally these overvoltages are obtained by Multiconductor Transmission Line Theory using only part of one phase of the stator winding by applying a surge at the line-end coil. Moreover, many works consider the feeding cable to analyze only the voltage at machine terminals by using a simple model for the motor. This paper analyses the influence of the cable length on the transient voltage distribution inside the machine by numerical simulations using a three-phase model for the machine windings. The results are obtained by a cable-motor model using Finite Elements Method (FEM). The model couples the transient magnetic fields solved in a 2D geometry with electric circuit elements. Results show that the cable length has influence on the transient voltage distribution, especially for the line-end coils from the phase where the surge has been applied to.**

***Keywords*: Cable Transient Model, Electrical Machines, Transient Voltage Distribution, Finite Elements Method (FEM).**

I. Introduction

THE study of transient voltage distribution in electrical machines has become more important after the development of power electronics and the advance of PWM (Pulse Width Modulation) frequency converters. The short rise time of the pulses generated by these kind of converters exposes the machine windings to high overvoltages [1]-[3]. Moreover, even in electrical systems with motors not driven by frequency converters, a short rise time can be generated, for example, by lightning discharges, intermittent ground faults and circuit breaker switching during motor energization or interruption of the motor starting.

The most common model used in the literature to obtain the interturn (turn-to-turn and turn-to-ground) voltages uses the Multiconductor Transmission Line Theory (MTLT) [4]-[6], in which each turn of the machine is considered as a conductor of a transmission line crossing different medias, stator-core and end-windings. Normally, the model uses only one or two coils from a single phase, being the remaining coils represented by an equivalent resistance [6]. However, to consider all the reflections due to the mismatch impedances between the coils from the same and from the different phases, a three-phase model is required.

Moreover, there are also many studies that investigate the influence of the cable length on the transient voltage, especially at the motor terminals. Nevertheless, in these studies the machine is modelled by a simple model, using, for example, a surge impedance or a fitted frequency response [7][8].

In this sense this paper aims to verify the influence of the cable length on the transient voltage inside the machine using a three-phase model for the motor. In this model the transient magnetic fields and electric circuit elements (lumped parameters) are coupled [9][10]. Finite Elements Method is used to obtain the electric parameters and to perform the transient simulations. With this approach it is also possible to consider the cable model as electric circuit elements and perform the transient analysis in a single solution.

The main contributions of the paper are: a three-phase model is used to obtain the transient voltage distribution inside the machine windings and; integration of the cable-motor models in the same FEM solution.

II. Cable Model

The numerical results presented in this paper for the set cable/motor have been obtained by FEM simulations performed in Ansys Maxwell software. The cable has been modeled by lumped elements, that is, as electric circuit elements. The model used is based on previous works [11][12], which considers the frequency dependence of the series impedance and shunt admittance. The basic circuit for each meter of cable can be seen in Fig. 1. The model consists in fitting the frequency responses of the series impedance and the shunt admittance.

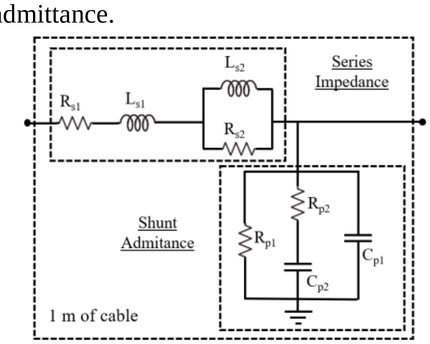

Fig. 1. Model of the cable.

This work was partially supported by INERGE (Instituto Nacional de Energia Elétrica), CNPq (Conselho Nacional de Desenvolvimento Científico e Tecnológico), CAPES (Coordenação de Aperfeiçoamento de Pessoal de Nível Superior) Finance Code 001 and FAPEMIG (Fundação de Amparo à Pesquisa do Estado de Minas Gerais).

R. S. Ferreira and A. C. Ferreira are with the Department of Electrical Engineering, Universidade Federal do Rio de Janeiro, COPPE/UFRJ, Rio de Janeiro, Brazil (e-mail: rodrigo.sousa@ufrj.br and ferreira@ufrj.br).

Paper submitted to the International Conference on Power Systems Transients (IPST2021) in Belo Horizonte, Brazil, June 6-10, 2021.

In the original model the parameters presented in Fig. 1 are calculated based on the measured open-circuit and short-circuit impedances as a function of frequency. However, in the present paper they are obtained based on the frequency response of the series impedance and shunt admittance, which are calculated by FEM simulations. Therefore, the first step to achieve the transient model is to build the cable geometry. The main data of the cable used is presented in TABLE I and the geometry implemented can be seen in Fig. 2.

TABLE I
PARAMETERS USED TO CALCULATE THE CAPACITANCES.

Parameter	Value
Type	Three-Core
Number of individual conductors	19
Conductor diameter [mm]	12.2
Insulation thickness [mm]	4.5
Inner sheath diameter [mm]	58.3
Insulation Material	EPR

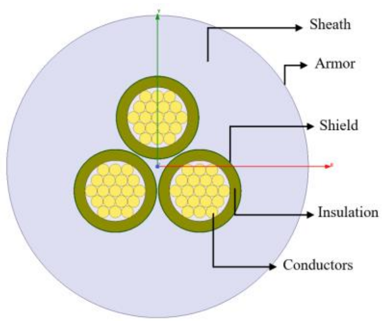

Fig. 2. Geometry of the cable.

The parameters (inductance, resistance, conductance and capacitance) of the cable are extracted using a frequency dependent solver in FEM software. The range of frequencies used were considered according to the frequency spectrum of the applied signal. Therefore, the lowest and highest frequencies were chosen according to the FFT (Fast Fourier Transform) of the surge applied in the sending end of the cable, which in this paper is a simple ramp that can be considered as a single trapezoidal pulse.

The frequency spectrum of a single trapezoidal pulse depends on the rise time (t_{rise}), but, in general, the frequency response has a maximum magnitude for 0 Hz (DC signal) and the maximum frequency is approximately equal to $1/t_{rise}$. For this paper, to model the electrical cable, the range of frequency considered is from 0 Hz to 10 MHz, which is suitable to consider the frequency content of the applied surge.

After calculating the frequency responses, the series impedance and shunt admittance can be fitted. The procedure to calculate the parameters of the series impedance and shunt admittance, depicted by Fig. 1, is indicated as follows:

- R_{s1}: is the low-frequency resistance, that is, the resistance for the lowest frequency considered;
- R_{s2}: is the difference between the high-frequency resistance (resistance calculated for the highest frequency) and low-frequency resistance;
- L_{s1}: is the high-frequency inductance;
- L_{s2}: is the difference between the low and the high-frequency inductances;
- C_{p1}: is the high-frequency capacitance;
- C_{p2}: is the difference between the low-frequency and the high-frequency capacitances;
- R_{p1}: is the low-frequency conductance;
- R_{p2}: is the difference between high and low-frequency conductances.

Applying this procedure, the fitted series impedance and shunt admittance can be obtained. The comparison between the original (calculated by FEM as a function of the frequency) and the fitted curves can be seen from Fig. 3 to Fig. 6.

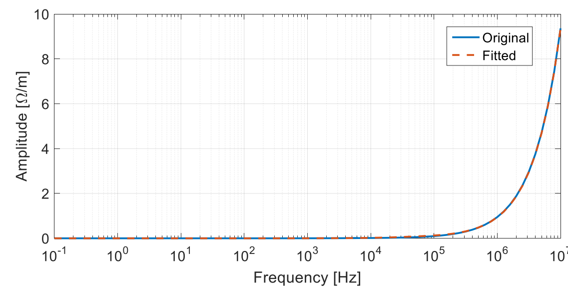

Fig. 3. Cable series impedance amplitude.

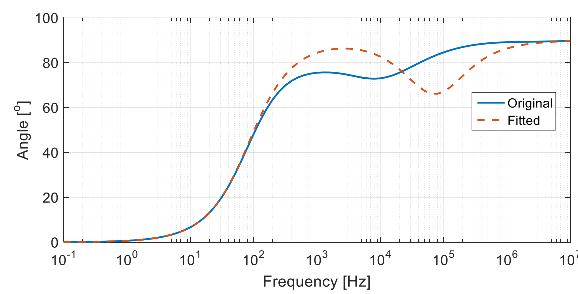

Fig. 4. Cable series impedance angle.

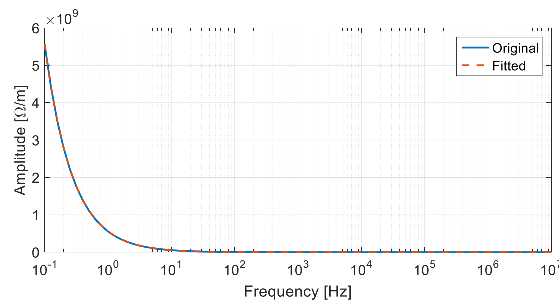

Fig. 5. Cable shunt admittance amplitude.

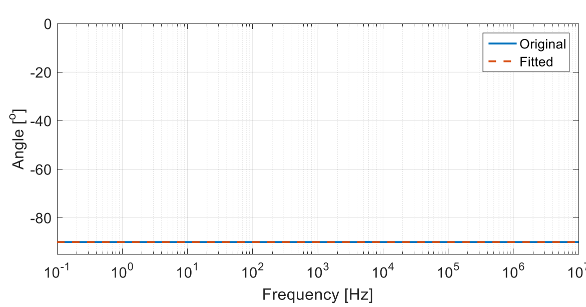

Fig. 6. Cable shunt admittance angle.

According to the previous figures, the cable model can be considered suitable, because the only relevant difference, between the original and the fitted models, has been found for the angle of the series impedance in intermediary frequencies. Therefore, the surge impedance amplitude of the cable, which affects the reflection factor, is less influenced by this divergence. The frequency responses would be better adjusted if more RLC parameters were used for the cable model. However, this approach requires more simulation time with little gain in accuracy.

III. Motor Model

The transient simulations are performed in a 2D geometry of the motor built in FEM software. The main data used during the studies can be seen in TABLE II.

TABLE II
Motor main data.

Type	Squirrel Cage Induction
Rated Power [MW]	10
Rated Voltage [kV]	13.8
Winding	Double Layer
Connection	Isolated Star
Number of Turns per Coil	13
Individual Conductors Size [mm x mm]	3.2 x 6.8
Main Insulation Thickness [mm]	3.0
Turn Insulation Thickness [mm]	0.3
Stator External Diameter [mm]	1580

The model used to obtain the transient voltage distribution inside the machine is better explained in a complementary paper [11], which can be understood by the equivalent circuit depicted by Fig. 7.

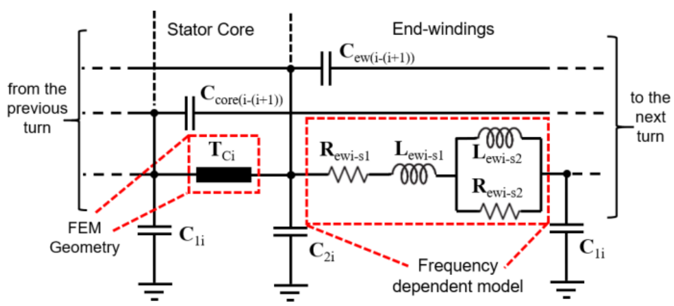

Fig. 7. Equivalent circuit for each stator turn.

In summary, each stator turn is modeled as two "π" sections composed of elements in which transient magnetic fields are directly solved by FEM and electric circuit elements

The 2D geometry of the stator core, indicated by $\mathbf{T}_{Ci}$ in Fig. 7 (where "i" is the i-th turn) is directly modeled in the FEM software. Furthermore, to include the electric field effects, the stray capacitances, for both regions, end-windings and stator-core, are included as electric circuit elements between the conductors of the 2D geometry.

According to Fig. 7, the capacitances considered are the turn-to-turn ($\mathbf{C}_{core(i-(i+1))}$ for the stator-core region and $\mathbf{C}_{ew(i-(i+1))}$ for the end-windings region) and the turn-to-ground ($\mathbf{C}_{1i}$ and $\mathbf{C}_{2i}$). Moreover, as a 2D geometry is considered, the series impedance for each turn of the end-windings is also considered as electric circuit elements, represented by $\mathbf{R}_{ew\text{-}s1}$, $\mathbf{R}_{ew\text{-}s2}$, $\mathbf{L}_{ew\text{-}s1}$ and $\mathbf{L}_{ew\text{-}s2}$.

The capacitances are calculated by a 2D geometry for the stator-core and by a 3D geometry for the end-windings, using an electrostatic solver. The frequency-dependent model for the series impedance of the end windings is calculated similarly to the series impedance of the cable, as explained in the previous section, which means that the resistance and inductance of each turn are obtained as a function of the frequency by an equivalent 2D geometry and, posteriorly, the parameters of the fitted model are calculated following the same procedure.

Therefore, the complete model for the set cable/motor is composed of the 2D geometry of the stator-core, where the transient magnetic equations are solved by FEM software, and electric circuit elements for the motor and cable models. The details of the calculation of the electric circuit elements for the machine model are presented in the complementary paper [11]. In this paper the rotor has not been considered, since the effect of the rotor can be neglected when the cable is considered.

IV. Model Validation

The explanation of the methodology used to validate both models, machine and cable, are presented in sequence.

A. Electrical Machine

The machine model explained in the last section is validated by comparing the calculated values with measurement results, which is presented in details in the complementary paper [11].

In summary, the capacitances-to-ground calculated by FEM are compared with measurement results for each coil. According to the results, the values has differed by 8.1%. Basically, the capacitances-to-ground of the electrical machine depends on the geometry and the relative permittivity values used for the insulations. Therefore, in the FEM model the dimensions of the conductors and insulation layers are well defined and constant. However, in a practical machine, the dimensions and the permittivity of the insulation materials vary, even for a very controlled manufacturing process. Therefore, considering the difficulty for controlling the exact dimensions and permittivity of the insulations, an 8.1% difference is considered suitable for the purpose of this paper.

Moreover, the transient waveform obtained by the FEM model is compared with the surge test [13] result, which has been performed for a single coil. To validate the transient model, the simulations should be compared with measurement results obtained by using the same procedure, which means that the turn-to-turn and turn-to-ground voltages should be measured by using the same applied surge. However, to measure these transient voltages in large machines, as the one used in this research, the main and turn insulations of the coils should be removed to be possible to access the turns at the measurement points. Therefore, the insulation would be damaged and the process to recovery it is complex and involve high costs. In this sense, due to the difficult in performing these tests in large machines and the costs involved, an alternative way to validate the high-frequency phenomena is to use a standard test, like the surge test, which is normally already preformed during the acceptance tests of the motor. The same high-frequency effects observed in the interturn transient voltages is captured by the surge test. As shown in [11], the simulated and measured results had good agreement.

B. Electrical Cable

To validate the geometry of the cable, the rated parameters informed by the manufacturer are compared with those obtained in FEM, which results are presented in TABLE III.

TABLE III
VALIDATION OF CABLE PARAMETERS.

Parameter	Rated	Calculated	Error
DC Resistance [mΩ/m]	0.195	0.189	3.0
Inductance @60 Hz [μH/m]	0.345	0.351	1.7
Capacitance [ηF/m]	0.290	0.286	1.3

Since the geometry of the cable has been validated, it is considered not necessary to validate the transient model, because it is well validated in the literature [11][12].

V. TRANSIENT SIMULATIONS

Numerical simulations were performed using the model described in the previous sections to verify the cable influence on the turn-to-turn and turn-to-ground voltages, since they stress the turn and main insulations, respectively. The motor used is composed of 24 coils per phase, which form 4 groups of six coils each. The simulations consider one group of coils. The surge is applied in the line-end coil of phase "a" and the line-end coils of phases "b" and "c" are grounded, as shown in Fig. 8, because it is considered that the surge achieves the phase "a" of the cable and it propagates to the machine. To focus only on the effects generated by the surge, using the superposition theorem, the normal sources (the sinusoidal ones) can be short-circuited and, for phases "b" and "c", they can be also grounded.

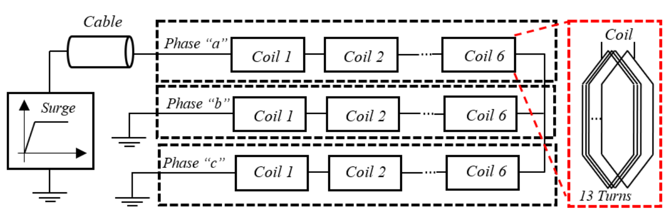

Fig. 8. Setup of the simulations.

For the cable, only one phase has been considered, since the influence of the other phases can be neglected, because the reflections occurred in the junction machine/cable of phases "b" and "c" are well damped due to the propagation time needed for the surge to return to phase "a" (which presents the highest overvoltages). Therefore, a considerable time is saved without losing precision.

The simulations have been performed using a simple ramp function with amplitude (V_{AP}) equal to 100 V and a rise time equal to 0.2 μs. This type of the pulse has been chosen because the main parameter which affects the overvoltages inside the motor is the rise time, which can be easily changed in a ramp waveform. Moreover, 0.2 μs is the front time of the standard waveform to model lightning impulses and also a typical value used in this kind of studies.

The objective is to compare the transient voltages without the cable with different cable lengths, for instance, 20 m, 50 m, 100 m and 200 m, for all the turns of the three phases, which means that the voltages for the 78 turns of each phase are presented. All results are in the percentage of the applied voltage (% of V_{AP}). The cable lengths used in the simulations are typical values for industrial applications, which can vary from few meters to some hundreds of meters.

In sequence, the transient results are presented. Firstly, the importance to consider a three-phase mode for the machine is discussed and, posteriorly, the terminal and internal voltages are analyzed considering the cable influence.

A. Three-Phase Model

The most common models to study transient voltage distribution inside the machine windings use only one or two coils from a single phase, being the remaining coils represented by an equivalent resistance. However, to consider all the reflections due to the mismatch impedances between the coils from the same and from different phases, a three-phase model is required. Fig. 9 and Fig. 10 show the turn-to-turn and turn-to-ground voltages obtained from simulation results (peak values in the percentage of the amplitude of the applied surge) for the turns belonging to the first coil, when applying a surge with a rise time equal to 0.2 μs at the machine terminals, considering different models, for instance, 1) three-phase model for one winding group (used in this paper); 2) one-coil model; 3) one-coil model with the remaining coils represented by a resistance of 100 Ω and; 4) one complete phase model from one winding group.

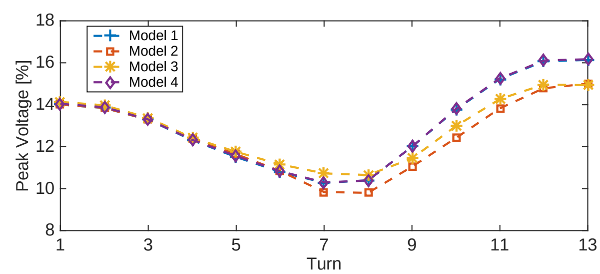

Fig. 9. Turn-to-turn results comparison for different models.

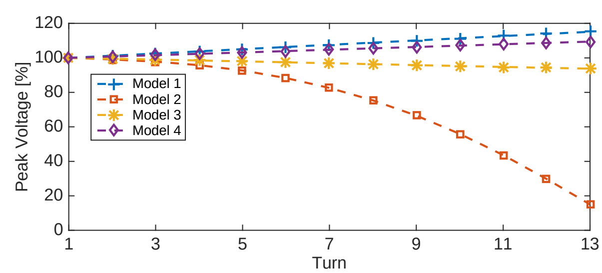

Fig. 10. Turn-to-ground results comparison for different models.

According to the previous figures, the peak values found for simpler models are different for both, turn-to-turn and turn-to-ground voltages, leading to underestimated results, since the maximum values are found for the three-phase model. Regarding the one-phase model, the turn-to-turn peak values are quite similar, however, the turn-to-ground voltages are still underestimated. Therefore, if a model other than the three-phase one is used, the insulation design could be undersized. For this reason, a three-phase model for the machine is used in this paper to verify the cable influence on the internal overvoltages.

B. Cable influence on the Terminal Voltages

In this subsection the terminal voltages, that is, in the cable receiving end, are presented for cases that consider and neglect the motor model. In Fig. 11 and Fig. 12 the waveforms are compared for the shortest and longest cable simulated, respectively. Moreover, in TABLE IV is presented the comparison between the peak values and the rise time of the voltages at the cable receiving end, for both cases, with and without the motor.

According to the figures it is evident the reduction of the amplitude and oscillation frequency when the motor is considered. One interesting observation can be taken from the waveform for the cable of 200 m that shows little peaks superposed, which are related to the reflections in the line-end coil due to the mismatch impedance in the stator core-end windings junctions.

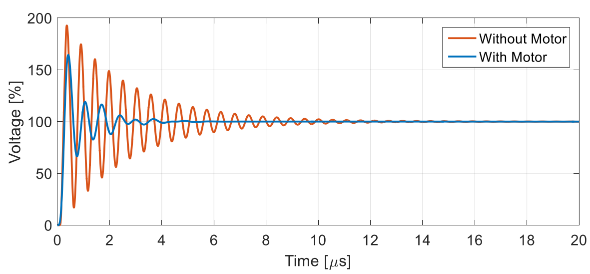

Fig. 11. Motor terminal voltage for cable of 20 m.

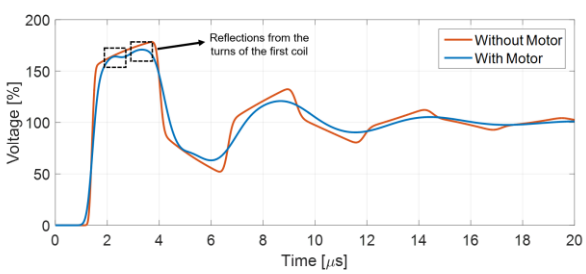

Fig. 12. Motor terminal voltage for cable of 200 m.

TABLE IV
MAXIMUM TURN-TO-GROUND VOLTAGES.

Cable length [m]	Without Motor		With Motor	
	Peak [%]	Rise time [μs]	Peak [%]	Rise time [μs]
20	192.8	0.16	164.4	0.20
50	188.9	0.17	179.8	0.28
100	182.9	0.20	181.6	0.42
200	178.3	0.59	170.8	0.64

According to the results, the peaks increase with the cable length, except for the case of 200 m, which has presented lower values for both cases. In relation to the rise time, they increase with the cable length for both, with and without the motors. Nevertheless, when the motor is considered the increasing is still higher. This is an important observation to understand the turn-to-turn and turn-to-ground voltages presented in the next section, which is the main purpose of the simulations in this subsection. Moreover, the previous figures also aimed to show that depending on the set cable/motor, oscillations can be produced by the reflections occurring in the turns of the first coils. Therefore, a simpler model, which does not consider the turns individually, cannot detect properly these oscillations.

C. Cable influence on the Internal Voltages

In this subsection the transient voltage distribution between turns and from turns-to-ground are presented for different cable lengths. The voltage waveforms are presented only for phases “a” (where the surge has been applied to) and “b” because in phase “a” it is where the highest overvoltages are found and the results for phases “b” and “c” are similar. However, the peak values are compared for the three phases. The turn-to-turn and turn-to-ground waveforms are presented from Fig. 12 to Fig. 20, which are related to the last turns within each coil.

The waveforms are a result of the interaction of many reflected waves occurring in the junctions, for instance, in the cable-motor, in the same coil within the motor (stator-core/end-windings/stator-core) and in the star-point connection.

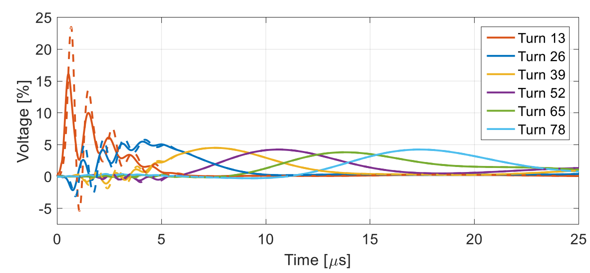

Fig. 13. Turn-to-turn voltages for phase “a” (without cable: solid lines and with cable of 20 m: dashed lines).

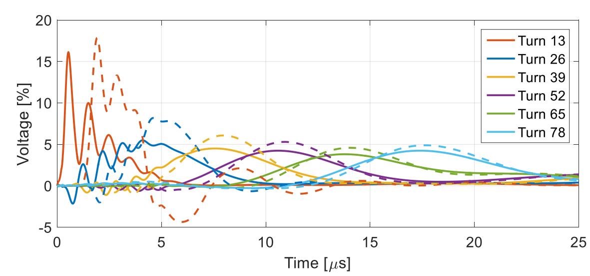

Fig. 14. Turn-to-turn voltages for phase “a” (without cable: solid lines and with cable of 200 m: dashed lines).

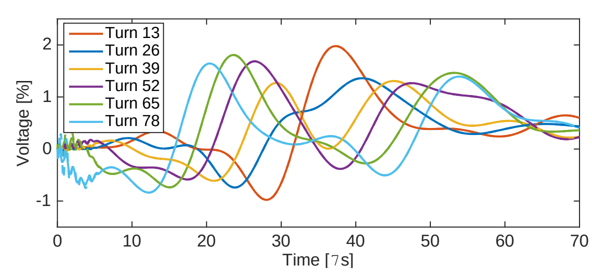

Fig. 15. Turn-to-turn voltages for phase “b” (without cable: solid lines and with cable of 20 m: dashed lines).

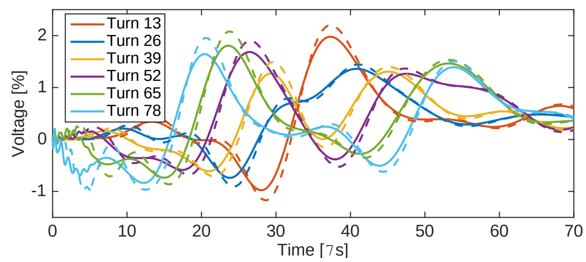

Fig. 16. Turn-to-turn voltages for phase “b” (without cable: solid lines and with cable of 200 m: dashed lines).

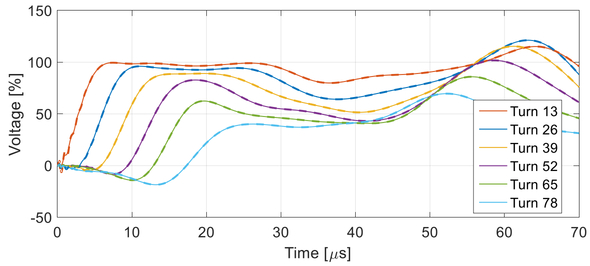

Fig. 17. Turn-to-ground voltages for phase “a” (without cable: solid lines and with cable of 20 m: dashed lines).

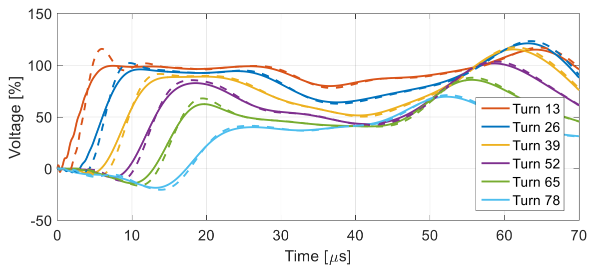

Fig. 18. Turn-to-ground voltages for phase “a” (without cable: solid lines and with cable of 200 m: dashed lines).

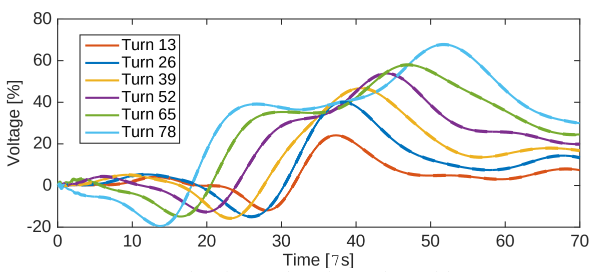

Fig. 19. Turn-to-ground voltages for phase “b” (without cable: solid lines and with cable of 20 m: dashed lines).

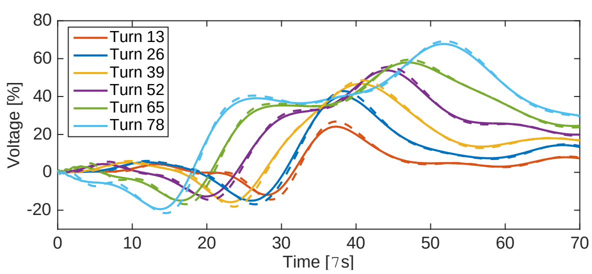

Fig. 20. Turn-to-ground voltages for phase “b” (without cable: solid lines and with cable of 200 m: dashed lines).

According to the figures, it can be noted that for the lowest cable length (20 m) the cable has influence only in the first two turns presented, which belong to the first 2 line-end coils, whereas for the longest cable (200 m) the amplitudes have been changed for all turns. The main explanation can be obtained by the waveforms presented previously in Fig. 11 and Fig. 12, which show that for shorter cable lengths the oscillation at the motor terminals finishes before. For instance, the oscillation finishes after about 5 µs for the cable of 20 m. For the turn-to-ground results, relevant differences have been found only for longer cables for the first turns.

To verify the influence of the cable length in all the three phases, from Fig. 21 to Fig. 26 the voltage peaks are presented for all the lengths simulated, considering both results, turn-to-turn and turn-to-ground. For the turn-to-turn results, it can be noted that for the turns belonging to the first coil (1^{st} to 13^{th}) the voltages are as higher as shorter is the cable, which is explained by the fact that for shorter cable lengths the rise time of the voltage at the machine terminals are lower, therefore, lower rise times imply to higher turn-to-turn voltages. For the turns from the third coil of phase “a” and for all turns of phases “b” and “c”, higher values are found for longer cables, but the variations are lower than for the first turns.

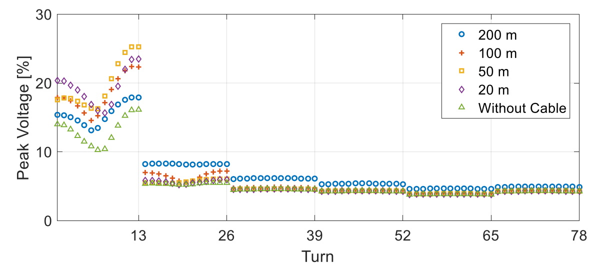

Fig. 21. Turn-to-turn peak voltages for phase “a”.

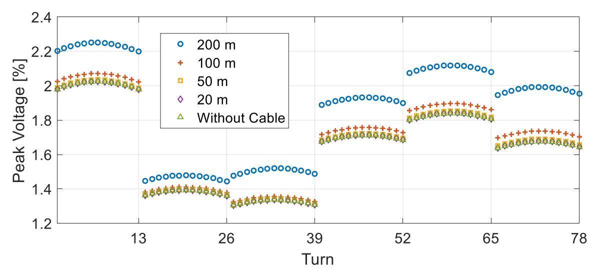

Fig. 22. Turn-to-turn peak voltages for phase “b”.

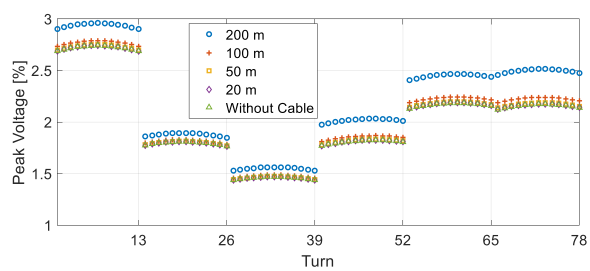

Fig. 23. Turn-to-turn peak voltage voltages for phase “c”.

For the turn-to-ground results, the main observation is that the cable has significant influence only on the voltages of the first turns of the first coil for the phase where the surge has been applied to. It can be also seen that the highest result is observed for the first turn of the 100 m cable. Nevertheless, in general, for the first coil the highest results are observed for the cable of 50 m and they do not have a relation with the length of the cable, because they depend on the reflections that occur due to the mismatch impedance in the stator core-end windings junctions in the first coil. For the turns belonging to the coils other that the first of phase "a" and all turns of phases "b" and "c", again, the voltages are as higher as longer are the cable, however, lower variations are observed when compared with the turn-to-turn ones.

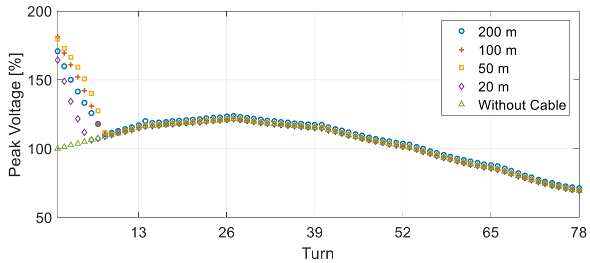

Fig. 24. Turn-to-ground peak voltages for phase "a".

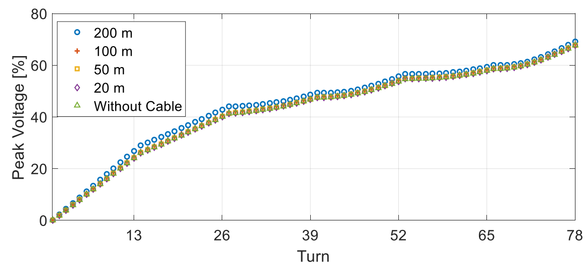

Fig. 25. Turn-to-ground peak voltages for phase "b".

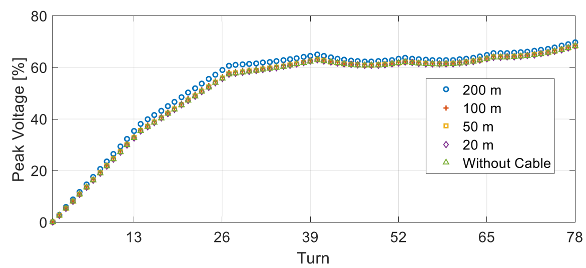

Fig. 26. Turn-to-ground peak voltages for phase "c".

VI. Conclusions

This paper presents the influence of the cable length on the three-phase transient voltage distribution in rotating machine stator windings. The proposed model considers all coils of one winding group from the three phases, which is not found in the literature, since the turn-based models normally used only consider part of the winding. The model also allows us to obtain the voltage at the terminals and inside of the machine, which is required to know the correct overvoltages. The model of each individual coil has been validated by experimental results in a complementary paper. Moreover, the geometry of the cable has also been validated by the manufacturer data.

Simulations aimed to verify the influence of the cable length on the turn-to-turn and turn-to-ground transient overvoltages, which are important to design the turn and main insulations, respectively. According to the results, for shorter cables, the influence is seen only in the first line-end coils for the phase which the surge has been applied to, nevertheless, for longer cables the amplitude is changed for all turns from the three phases.

Regarding the turn-to-turn results, the maximum values are found for the shortest cables, since in these cases the rise time of the voltage at machine terminal is lower.

In relation to the turn-to-ground results, the main observation is that the cable has significant influence only on the voltages of the first turns of the first coil for the phase where the surge has been applied to. Moreover, it was not found a rule for the highest voltage as a function of the cable length, because the values depend on the reflections that occur due to the mismatch impedance in the stator-core/end-windings junctions in the first turns of the line-end coil.

Normally, surge capacitors are used to reduce the rise time of the voltage that penetrates into the machine windings, hence turn-to-turn overvoltages are lower. These capacitors are chosen according only to the machine rated voltage. Based on the results, for longer cables the turn-to-turn voltages are lower due to the reduction of the rise time, which suggests that lower surge capacitors could be used.

VII. References

[1] S. Amarir and K. Al-Haddad, "A Modeling Technique to Analyze the Impact of Inverter Supply Voltage and Cable Length on Industrial Motor-Drives," in IEEE TPEC, vol. 23, no. 2, pp. 753-762, March 2008.

[2] P. Bidan, T. Lebey, G. Montseny and J. Saint-Michel, "Transient voltage distribution in inverter fed motor windings: experimental study and modeling," in IEEE TPEC, vol. 16, no. 1, pp. 92-100, Jan. 2001.

[3] H. A. Toliyat, G. Suresh and A. Abur, "Estimation of voltage distribution on the inverter fed random wound induction motor windings supplied through feeder cable, " in IEEE TEC, vol. 14, no. 4, pp. 976-981, Dec 1999.

[4] Zhang et al., "Analysis of Inter-Turn Insulation of High Voltage Electrical Machine by Using Multi-Conductor Transmission Line Model," in IEEE TMAG, vol. 49, no. 5, pp. 1905-1908, May 2013.

[5] H. De Gersem, O. Henze, T. Weiland and A. Binder, "Transmission-line modelling of wave propagation effects in machine windings," 13th International Power Electronics and Motion Control Conference, Poznan, 2008, pp. 2385-2392.

[6] M. K. Hussain and P. Gomez, "Modeling and Experimental Analysis of the Transient Overvoltages on Machine Windings Fed by PWM Inverters," International Conference on Power Systems Transients (IPST 2017), Seoul, 2017.

[7] K. Jia, et al. "Modelling an AC motor with high accuracy in a wide frequency range," IET EPA, v. 7, n. 2, p. 116-122, 2013.

[8] A. F. Moreira, T. A. Lipo, G. Venkataramanan and S. Bernet, "High-frequency modeling for cable and induction motor overvoltage studies in long cable drives," in *IEEE TIAS*, vol. 38, no. 5, pp. 1297-1306, Sept.-Oct. 2002.

[9] W. N. Fu, P. Zhou, D. Lin, S. Stanton and Z. J. Cendes, "Modelling of solid conductors in two-dimensional transient finite-element analysis and its application to electric machines" in IEEE TMAG Magnetics, vol. 40, no. 2, pp. 426-434, March 2004.

[10] R. S. Ferreira and A. C. Ferreira, "Transient Voltage Distribution in Induction Motor Stator Windings Using Finite Elements Method," IECON 2018, Washington, DC, 2018, pp. 737-742.

[11] R. S. Ferreira and A. C. Ferreira, "Transient Model to Study Voltage Distribution in Electrical Machine Windings Considering the Rotor", Electric Power Systems Research, Volume 195, 2021.

[12] L. Wang, C. Ngai-Man Ho, F. Canales and J. Jatskevich, "High-Frequency Modeling of the Long-Cable-Fed Induction Motor Drive System Using TLM Approach for Predicting Overvoltage Transients," in *IEEE TPEC*, vol. 25, no. 10, pp. 2653-2664, Oct. 2010.

[13] IEEE Std 522, "Guide for Testing Turn-to-Turn Insulation on Form-Wound Stator Coils for Alternating-Current Rotating Electric Machines," 2004.